*Geosciences and Engineering, Vol. 8, No. 13 (2020), pp. 20–32.*

# SERIES EXPANSION BASED TAU-TRANSFORMATION WITH APPLICATION TO TDIP DATASET

BYAMBASUREN TURTOGTOH[1, 2] – MIHÁLY DOBRÓKA[1]

[1]*Department of Geophysics, University of Miskolc, Hungary,*
[2]*Research Institute of Applied Earth Sciences, University of Miskolc, Hungary*
*gfbyamba@uni-miskolc.hu*

**Abstract:** Geophysical data processing in the TDIP has shown itself to be an important and effective tool in ore exploration. The recovered images from the induced polarization (IP) survey are interpreted by geologists to understand the near-surface geological structures and to guide further exploration activities such as spotting drill holes. However, it does not always provide an exact near-surface image that reliably reflects the structural and physical properties of the target for many reasons. This paper aims to investigate the combination between the TAU transformation and the series expansion inverse method based on the overdetermined inverse problem (linearized Gaussian least squares method) in the data analysis of IP data. We also developed a stable algorithm to solve TAU transformation through the overdetermined problem (GLSQ). In this algorithm, the series expansion technique and a logarithmic transformation have been extended to define the unknown parameters. This algorithm is useful for the quick processing of TDIP data and may assist in accuracy improvement of the interpretation of a geoelectric survey in ore exploration.

***Keywords:*** *Time Domain Induced Polarization (TDIP), TAU transformation, series expansion, time constant spectrum*

## 1. INTRODUCTION

Interpretations and subsequent decision-making processes can be done more conveniently and potentially more reliably if they are based on geophysical data analysis. Geophysical data analysis methodology has become an effective and standard tool for interpreting geophysical surveys in ore exploration, engineering groundwater and environmental applications. These were developed by many scientists and mathematicians with various datasets and goals [1–5]. Nevertheless, the mathematical techniques do not represent subsurface structure well for many reasons: the non-uniqueness of mathematical solutions, limitations imposed by underlying physics, incomplete data coverage, limited measurement, technical problems, noise in the field data, etc. Despite all the progress that has been made in the direction of reducing the model uncertainty and enhancing the developing interpretation of the geophysical data processing, there are still some open questions and challenges to be addressed. Those problems are directly impacted to the data processing of time-domain induced polarization (TDIP) [6–7]. In a broader perspective, our research is more focused on time domain induced polarization. TDIP has many applications, not only in ore exploration – principally of disseminated sulphides – but also in connection with geotechnical engineering and environmental problems [8–12]. Several solutions using mathematical tools (the TAU transformation, the Gaussian least square method, the expansion coefficient, the logarithm transform) are being used in order to develop this area. TAU transformation was introduced by Turai in 1985 [13] for the interpretation of IP data. Induced polarization measurements are widely used in ore exploration. The TAU transformation was developed to process time-domain induced polarization datasets measured in a Schlumberger electrode array. In addition, a serious expansion inversion method has been confirmed for successful applicability by researchers in-field application and laboratory measurements [14–18]. In the study is more focused on development of the geoelectric method for ore exploration (with special emphasis on the solution of forwarding and inverse problems). The development of forwarding and inverse modelling methods play an important role in the advanced geophysical data processing. As well as, the combination of the TAU transformation and series expansion coefficient method. It is shown that the quality of inversion results is characterized by the distance between the measured data and those the calculated using the inverted time constant spectrums (Pole-dipole in TDIP). The inversion technique is tested on field measurements dataset of the Yamaat Yamaat gold deposit in the Republic of Mongolia. Our dissection aims to apply a combination of data processing and inversion tools to develop new methods of scientific value. The result of the novel methods will be tested by using field data sets to examine its validity.

## 2. METHODOLOGY

The so-called overdetermined inversion method (when the *N* number of measurement data is greater than the M number of unknown model parameters) is more frequently used in inversion. To solve the TAU-transformation problem, the overdetermined inverse problem theory can be successfully used [4]. The starting point is *Equation (1)* governing the forward problem:

$$\eta_a(t) = \int_o^{\infty} w(\tau) e^{-t/\tau} d\tau, \tag{1}$$

where $t$ is the time after turning off the excitation current, $\tau$ is the time-constant, and $w(\tau)$ is the time-constant spectrum, and the series expansion inversion method [14] (developed at the Geophysics Department) was applied. In constructing a general algorithm for the determination of the TAU transformation we write the $w(\tau)$ spectrum function in the form of series expansion

$$w(\tau) = \sum_{q=1}^{Q} B_q \, \Phi_q(\tau), \tag{2}$$

and the forward problem is formulated as

$$\eta_k^{calc} = \sum_{q=1}^{Q} B_q \, G_{kq}, \tag{3}$$

with the Jacobi matrix

$$G_{kq} = \int_o^\infty \Phi_q(\tau) e^{-t_k/\tau} d\tau. \tag{4}$$

The next step in formulating the inverse problem is introducing the deviation vector between measured and the calculated data

$$\vec{e} = \vec{\eta}^{meas} - \vec{\eta}^{calc} = \vec{\eta}^{meas} - \underline{G}\vec{B}, \tag{5}$$

where $\vec{\eta}^{meas}$is an apparent chargeability measured, $\vec{\eta}^{calc}$ an apparent chargeability calculated data, $\underline{\mathrm{G}}$ is Jacobi matrix and $\vec{B}$ is expantion coefficient.

In the framework of the Gaussian least squares method the $L_2$ norm $E=\|\vec{e}\|$ is minimized, resulting in the normal equation

$$\underline{G}^T \underline{G} \, \vec{B} = \underline{G}^T \vec{\eta}^{meas}, \tag{6}$$

with the solution

$$\vec{B} = (\underline{G}^T \underline{G})^{-1} \underline{G}^T \vec{\eta}^{meas}, \tag{7}$$

in the above algorithm, the positivity of the spectral amplitudes is not ensured. To fulfill this requirement, we used the transformation

$$b_q = \log(B_q), \tag{8}$$

resulting in the nonlinearity of the series expansion

$$w(\tau) = \sum_{q=1}^{Q} \exp\,(b_q)\, \Phi_q(\tau), \tag{9}$$

and the forward modeling equation  formulae

$$\eta(t_k) = \sum_{q=1}^{Q} \exp(b_q) \int_0^\infty \Phi(\tau) \exp\left(-\frac{t_k}{\tau}\right) d\tau. \tag{10}$$

Using the standard linearization procedure, we derived the normal equation of the Gaussian least squares

$$\underline{G}^T \underline{G}\, \delta\vec{b} = \underline{G}^T \delta\vec{\eta}, \tag{11}$$

with the solution

$$\delta\vec{b} = (\underline{G}^T \underline{G})^{-1} \underline{G}^T \delta\vec{\eta}, \tag{12}$$

and the updating formula

$$\vec{b}^{new} = \vec{b}^{old} + \delta\vec{b}. \tag{13}$$

It was observed that the Jacobi matrices belonging to the transformed (nonlinear) and the original (linear) algorithms are related as

$$G_{kj}^{nonlin} = B_j G_{kj}^{lin}, \tag{14}$$

this algorithm will be used in the inversion of the IP data set measured along Line_2 infield area of the field measurement sector in Mongolia shown in *Figure 1*.

## 3. TESTING ON FIELD MEASURED DATA

The measurement time vector is

$t$ = (0.28 0.36 0.44 0.52 0.6 0.68 0.76 0.84 0.92 1 1.08 1.16 1.24 1.32 1.4 1.48 1.56 1.64 1.72 1.8) in sec.

The time constant data are defined in various inversion tests with different dimension *M*. In all cases the minimal value of the time constant is $\tau_{min}$= 0.28 in sec, because there is no measurement data at an earlier time, andconsequently smaller time constants are not resolved. The maximal value of the time constant is under discussion, so it will be selected as $\tau_{max}$ = 5, $\tau_{max}$ = 10 and $\tau_{max}$ = 15 sec. The $\tau_i$ elements of time constant vector are determined by using the formula

$$q = (\tau_{\max}/t_{\min})^{(1/(M-1))},\ \tau_0 = \tau_{\max}/(q^M),\ \tau_i = \tau_0\, q^i,\ i = (1, \ldots, M), \tag{15}$$

ensuring a logarithmically equidistant set of $\tau_i$ within the given $\tau_{min}$ and $\tau_{max}$ at various *M* dimensions of the time constant vector (this is the number of unknowns). The quality of inversion results is characterized by the distance between the measured data and the calculated data using the inverted spectral amplitudes

$$D = \sqrt{\frac{1}{N}\sum_{k=1}^{N}(1 - \frac{\eta_k^{calc}}{\eta_k^{meas}})^2} * 100\%. \tag{16}$$

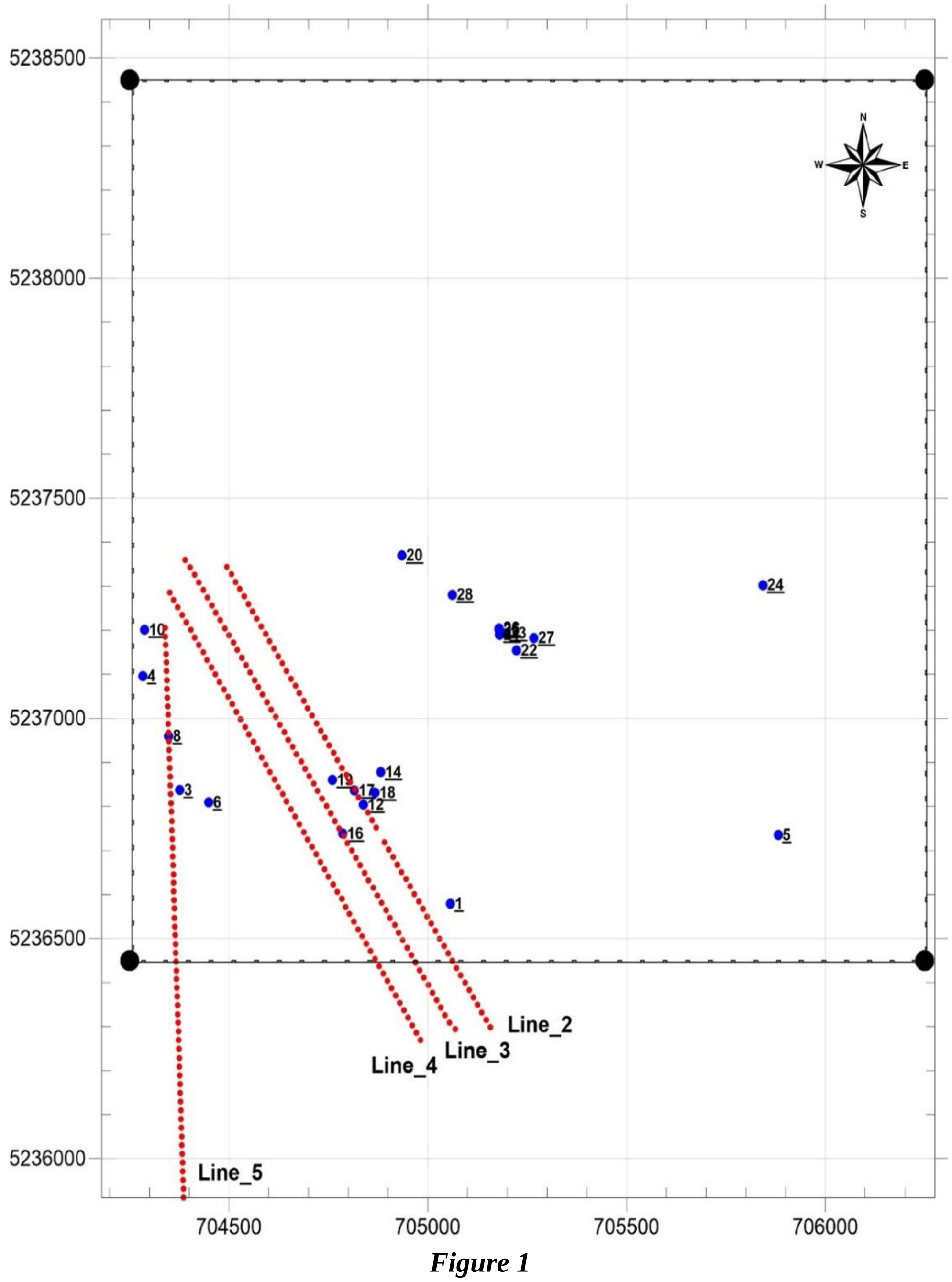


***Figure 1***

*The Yamaat gold deposit in location map, Mongolia. The pole-dipole profile from 2 to 4, drilled points (used for extracting core samples). The inside black square shows the research area of 2 × 2 km.*

In the first test of the overdetermined inversion algorithm on field data we choose again the apparent polarization data belonging to the first measurement point of Line 2:

$\eta_a$ = (7.66 6.92 6.18 5.77 5.26 4.64 4.36 4.1 3.87 3.61 3.47 3.35 3.16 3.02 2.85 2.68 2.71 2.56 2.34 2.29) in mV/V.

The results of the inversion are presented in *Table 1*.

***Table 1***

*The series expansion inversion results $\tau_{max}$ = 5 sec with various numbers of unknowns (M)*

| M | $\tau_i, w_i$ | 1 | 2 | 3 | 4 | 5 | 6 | 7 | 8 | 9 | 10 | D(%) |
|---|---|---|---|---|---|---|---|---|---|---|---|---|
| 10 | $\tau_i$ | **0.28** | **0.39** | 0.53 | 0.73 | 1 | 1.4 | **1.9** | **2.6** | 3.6 | 5 | 6.34 |
| | $w_i$ | **1.2** | **6.1** | 0.07 | 0.05 | 0.06 | 0.14 | **1.0** | **3.2** | 0.21 | 0.079 | |
| 9 | $\tau_i$ | **0.28** | **0.4** | 0.58 | 0.83 | 1.2 | 1.7 | **2.4** | 3.5 | 5 | | 6.35 |
| | $w_i$ | **1.9** | **5.5** | 0.06 | 0.05 | 0.07 | 0.24 | **3.9** | 0.39 | 0.11 | | |
| 8 | $\tau_i$ | **0.28** | **0.42** | 0.64 | 0.96 | 1.5 | **2.2** | **3.3** | 5 | | | 6.37 |
| | $w_i$ | **2.6** | **4.9** | 0.058 | 0.056 | 0.13 | **3.0** | **1.4** | 0.14 | | | |
| 7 | $\tau_i$ | **0.28** | **0.45** | 0.73 | 1.2 | **1.9** | **3.1** | 5 | | | | 6.39 |
| | $w_i$ | **3.2** | **4.4** | 0.064 | 0.1 | **1.8** | **2.6** | 0.12 | | | | |
| 6 | $\tau_i$ | **0.28** | **0.5** | 0.89 | 1.6 | **2.8** | 5 | | | | | 6.42 |
| | $w_i$ | **3.8** | **4.1** | 0.084 | 0.44 | **3.8** | 0.099 | | | | | |
| 5 | $\tau_i$ | **0.28** | **0.58** | 1.2 | **2.4** | 5 | | | | | | 6.46 |
| | $w_i$ | **4.6** | **3.7** | 0.091 | **3.2** | 0.87 | | | | | | |
| 4 | $\tau_i$ | **0.28** | **0.73** | **1.9** | **5** | | | | | | | 6.51 |
| | $w_i$ | **5.2** | **3.7** | **1.6** | **2** | | | | | | | |
| 3 | $\tau_i$ | **0.28** | **1.2** | **5** | | | | | | | | 6.64 |
| | $w_i$ | **6.4** | **4.6** | **1.9** | | | | | | | | |
| 2 | $\tau_i$ | *0.28* | *5* | | | | | | | | | *25.6* |
| | $w_i$ | *12.1* | *3.8* | | | | | | | | | |

It can be seen that 3 or 4 main polarization amplitudes at the relevant characteristic decay times appear at all choices of the number of unknowns. This feature can be observed in the tests with *M = (10, ..., 5)*. If we calculate the weighted average of the first two (bold) data

$$\hat{w}^k = \frac{w_1^k \tau_1^k + w_2^k \tau_2^k}{\tau_1^k + \tau_2^k}, k = (10,\ldots,5), \tag{17}$$

we find

$$\hat{w}^k = (4.05, 4.02, 3.98, 3.94, 3.99, 3.99),$$

which shows the existence of a characteristic polarization amplitude of $\hat{w} \approx 4.0$ in the [0, 0.6] sec decay time interval. A similar calculation shows another characteristic polarization amplitude

$$\hat{w}^k = (2.25, 2.43, 2.38, 2.55, 2.29, 2.57),$$

giving $\hat{w} \approx 2.41$ around $\hat{\tau} \approx 2.33$ sec.

The fit between the measured and the calculated data [using the $w(\tau_k)$ estimated spectral amplitudes in forward modeling] is similar for all tests (except that belonging to the non-physical *M = 2*). The fit is good even in the worst case of *M* = 3, as shown in *Figure 2*.

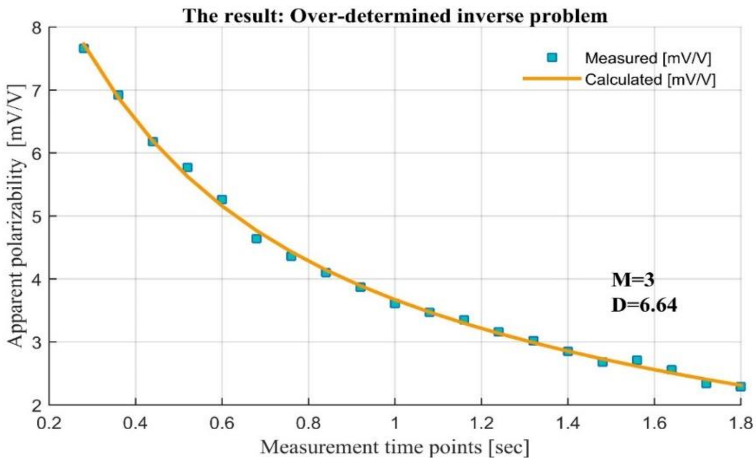


***Figure 2***

*The result of the series expansion inversion method: the measured and the calculated decay curve of apparent polarization at the first measurement point of Line_2: M = 3, $\tau_{max}$ = 5 in sec*

The inversion test was repeated with $\tau_{max}$ = 10 sec. The results are shown in Table 10. It can be seen again that 3 or 4 main polarization amplitudes appear at relevant characteristic decay times. This feature can be observed in the tests with *M = (10, ..., 5)*. We calculated the weighted average by using *Equation (17)*.
We find for the first two columns (bold)

$$\hat{w}^k = (3.98, 4.00, 3.98, 3.94, 3.95, 4.05),$$

which shows the existence of a characteristic polarization amplitude of $\hat{w} \approx 3.98$ in the [0, 0.68] sec decay time interval. A similar calculation shows another characteristic polarization amplitude at higher TAU values

$$\hat{w}^k = (2.08, 2.49, 1.90, 2.40, 3.27, 2.08),$$

giving $\hat{w} \approx 2.37$ around $\hat{\tau} \approx 2.89$ sec. It can be stated that the two main polarization amplitudes are nearly the same, as in the case of $\tau_{\max} = 5$ sec.

***Table 2***
*The series expansion inversion results using $\tau_{max}$ = 10 sec*
*with various numbers of unknowns (M)*

| M | $\tau_i, w_i$ | 1 | 2 | 3 | 4 | 5 | 6 | 7 | 8 | 9 | 10 | D(%) |
|---|---|---|---|---|---|---|---|---|---|---|---|---|
| 10 | $\tau_i$ | **0.28** | **0.42** | 0.62 | 0.92 | 1.37 | **2.04** | **3.04** | 4.52 | 6.72 | 10 | 6.37 |
| | $w_i$ | **2.42** | **5.02** | 0.06 | 0.05 | 0.12 | **2.45** | **1.82** | 0.15 | 0.06 | 0.04 | |
| 9 | $\tau_i$ | **0.28** | **0.44** | 0.68 | 1.07 | **1.67** | **2.62** | 4.09 | 6.4 | 10 | | 6.38 |
| | $w_i$ | **2.84** | **4.75** | 0.06 | 0.08 | **0.51** | **3.76** | 0.14 | 0.05 | 0.03 | | |
| 8 | $\tau_i$ | **0.28** | **0.78** | 1.30 | 2.16 | **3.60** | **6.00** | 10 | | | | 6.41 |
| | $w_i$ | **3.51** | **4.19** | 0.05 | 0.10 | **3.05** | **1.21** | 0.12 | 0.06 | | | |
| 7 | $\tau_i$ | **0.28** | **0.51** | 0.92 | **1.67** | **3.04** | 5.51 | 10 | | | | 6.43 |
| | $w_i$ | **3.95** | **3.94** | 0.08 | **1.11** | **3.11** | 0.09 | 0.04 | | | | |
| 6 | $\tau_i$ | **0.28** | **0.57** | 1.17 | **2.39** | 4.89 | 10 | | | | | 6.46 |
| | $w_i$ | **4.59** | **3.63** | 0.09 | **3.27** | 0.73 | 0.11 | | | | | |
| 5 | $\tau_i$ | **0.28** | **0.68** | **1.67** | **4.09** | 10 | | | | | | 6.50 |
| | $w_i$ | **5.06** | **3.64** | **1.28** | **2.41** | 0.08 | | | | | | |
| 4 | $\tau_i$ | **0.28** | **0.92** | **3.04** | 10 | | | | | | | 6.55 |
| | $w_i$ | **5.68** | **4.41** | **1.47** | 1.04 | | | | | | | |
| 3 | $\tau_i$ | 0.28 | **1.67** | 10 | | | | | | | | 6.81 |
| | $w_i$ | 7.02 | **5.86** | 0.46 | | | | | | | | |
| 2 | $\tau_i$ | 0.28 | 10 | | | | | | | | | 32.9 |
| | $w_i$ | 13.4 | 3.38 | | | | | | | | | |

The fit between the measured and the calculated data (using the $w(\tau_k)$ estimated spectral amplitudes in forward modeling) is similar for all tests (except that belonging to the non-physical *M = 2*) and the same as in *Figure 3*.

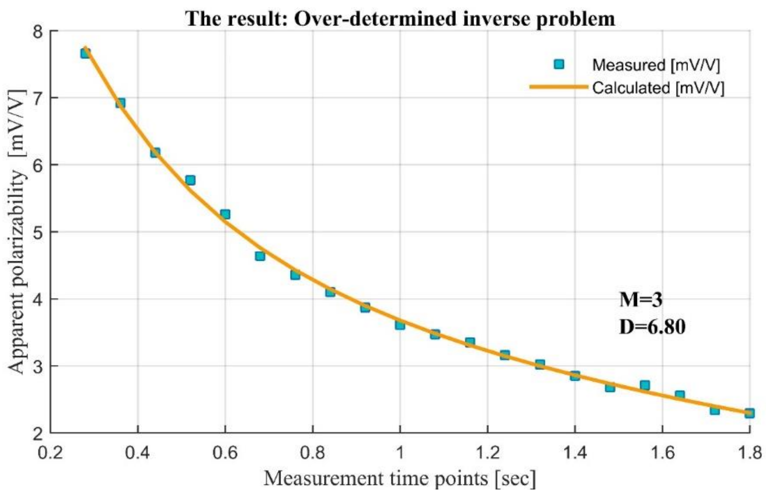


***Figure 3***
*Result of the series expansion inversion method: decay curve of the measured and the calculated apparent polarization at the first measurement point on the pole-dipole Line_2: M = 3 unknowns. $\tau_{max}$ = 10 sec*

Another inversion test was considered with $\tau_{\max} = 15$ sec. The results are shown in Table 3. It can be seen again that 3, 4 or 5 main polarization amplitudes appear at relevant characteristic decay times. This feature can be observed in the tests with *M = (10, …, 6)*. If we calculate the weighted average by using the previous equation,

$$\widehat{\mathrm{w}}^{\mathrm{k}} = (4.00, 3.93, 4.00, 3.90, 4.10),$$

which shows the existence of a characteristic polarization amplitude of $\widehat{\mathrm{w}}^{\mathrm{k}} \approx 3.99$ in the [0, 0.62] sec decay time interval.

***Table 3***

*The series expansion inversion results using $\tau_{max}$ = 15 sec with various numbers of unknowns (M)*

| M | $\tau_i, w_i$ | 1 | 2 | 3 | 4 | 5 | 6 | 7 | 8 | 9 | 10 | D(%) |
|---|---|---|---|---|---|---|---|---|---|---|---|---|
| 10 | $\tau_i$ | **0.28** | **0.44** | 0.68 | 1.06 | **1.64** | **2.56** | 3.98 | 6.19 | 9.64 | 15.0 | 6.37 |
| | $w_i$ | **2.82** | **4.76** | 0.06 | 0.08 | **0.42** | **3.85** | 0.15 | 0.06 | 0.04 | 0.03 | |
| 9 | $\tau_i$ | **0.28** | **0.46** | 0.76 | 1.25 | **2.05** | **3.37** | 5.54 | 9.12 | 15.0 | | 6.38 |
| | $w_i$ | **3.41** | **4.25** | 0.06 | 0.10 | **2.71** | **1.56** | 0.12 | 0.06 | 0.04 | | |
| 8 | $\tau_i$ | **0.28** | **0.49** | 0.87 | **1.54** | **2.72** | 4.81 | 8.49 | 15.0 | | | 6.41 |
| | $w_i$ | **3.76** | **4.13** | 0.08 | **0.41** | **3.78** | 0.10 | 0.04 | 0.03 | | | |
| 7 | $\tau_i$ | **0.28** | **0.54** | 1.06 | **2.05** | **3.98** | 7.73 | 15.0 | | | | 6.43 |
| | $w_i$ | **4.38** | **3.66** | 0.09 | **2.62** | **1.49** | 0.11 | 0.06 | | | | |
| 6 | $\tau_i$ | **0.28** | **0.62** | **1.38** | **3.05** | 6.77 | 15.0 | | | | | 6.46 |
| | $w_i$ | **4.74** | **3.80** | **0.27** | **3.50** | 0.08 | 0.04 | | | | | |
| 5 | $\tau_i$ | 0.28 | 0.76 | 2.05 | 5.54 | 15.0 | | | | | | 6.50 |
| | $w_i$ | 5.33 | 3.74 | 1.80 | 1.55 | 0.12 | | | | | | |
| 4 | $\tau_i$ | 0.28 | 1.06 | 3.98 | 15.0 | | | | | | | 6.55 |
| | $w_i$ | 5.87 | 5.02 | 0.66 | 1.11 | | | | | | | |
| 3 | $\tau_i$ | 0.28 | 2.05 | 15.0 | | | | | | | | 6.81 |
| | $w_i$ | 7.89 | 5.61 | 0.0003 | | | | | | | | |
| 2 | $\tau_i$ | 0.28 | 15.0 | | | | | | | | | 32.9 |
| | $w_i$ | 13.8 | 3.24 | | | | | | | | | |

A similar calculation shows another characteristic polarization amplitude at higher TAU values

$$\widehat{w}^k = (2.51, 2.00, 2.56, 1.79, 2.50),$$

giving $\widehat{w} \approx 2.27$ around $\hat{\tau} \approx 2.48$ sec. It can be stated that the two main polarization amplitudes are nearly the same, as in the case of $\tau_{\max} = 5$ sec and $\tau_{\max} = 10$ sec shown in *Figure 4*.

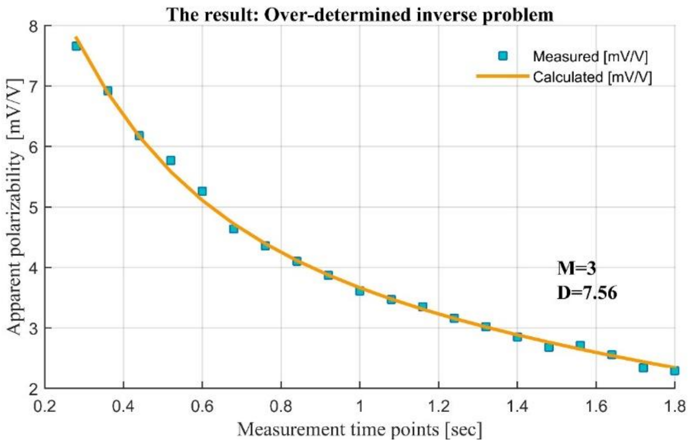


***Figure 4***

*Result of the series expansion inversion method: decay curve of the measured and the calculated apparent polarization at the first measurement point on the pole-dipole Line_2: M = 3* unknowns, $\tau_{max}$ = 15 sec

In the over-determined inverse problem, the fit between the measured and the calculated data (using the $w(\tau_k)$ estimated spectral amplitudes in forward modelling) is similar for all tests (except that belonging to the nonphysical $M$ = 2, and the physical from $M$ = 3 to $m$ = 10), as shown in *Figure 5*.

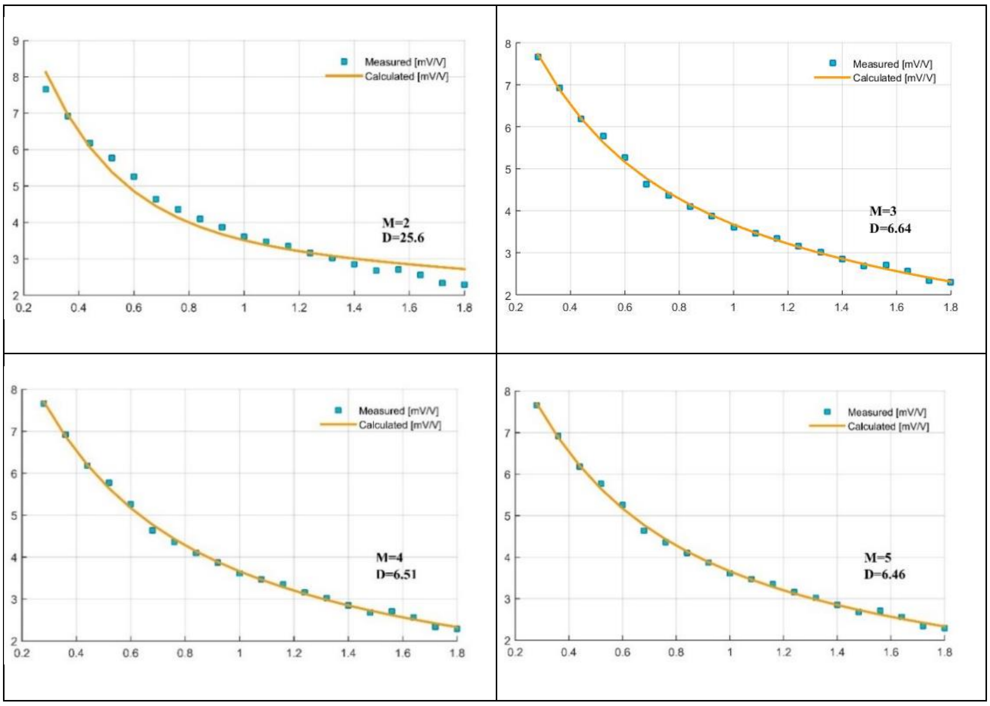

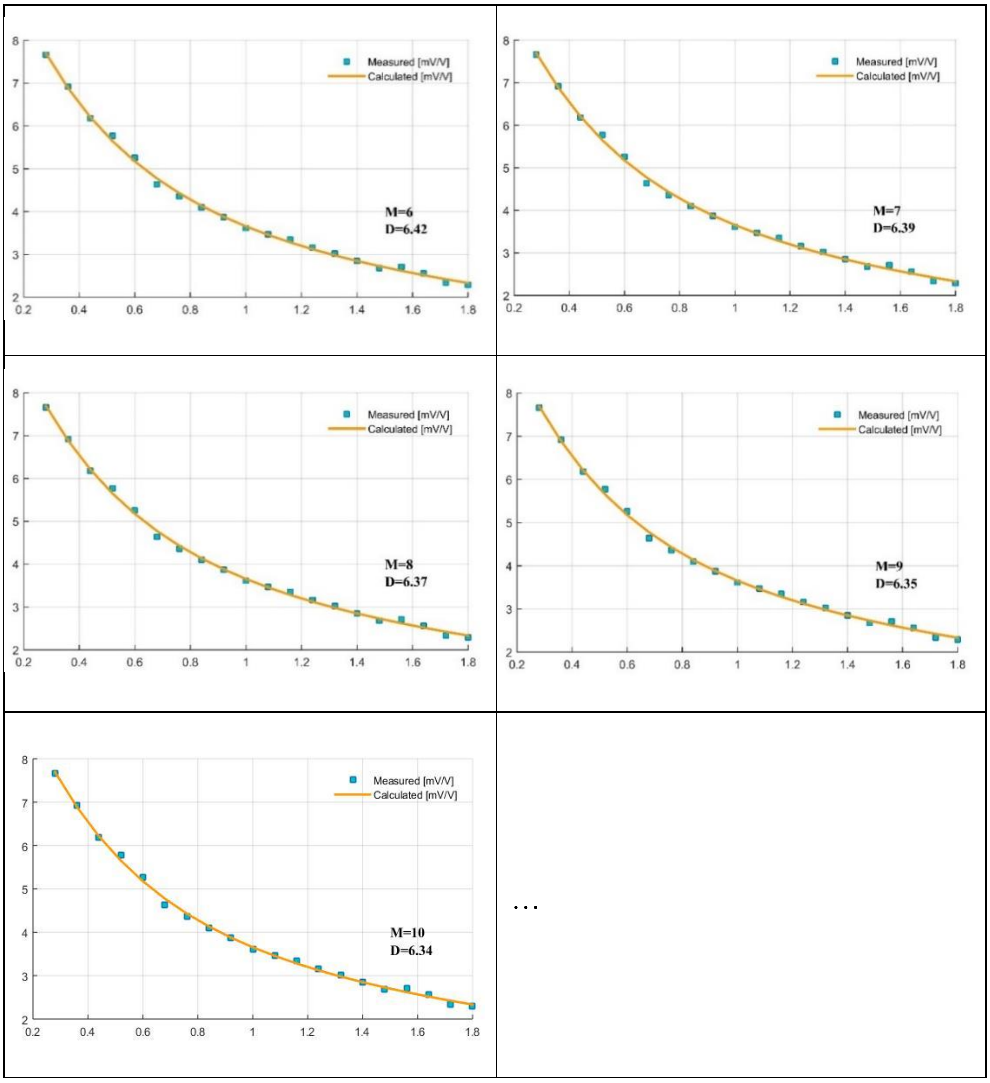


***Figure 5***
*Result of the series expansion inversion method: decay curve of the measured and the calculated apparent polarization at the first measurement point on the pole-dipole Line_2: from M = 2 to M = 10 unknowns, on horizontal axes the measurement time points (sec) and on vertical axes the apparent polarization (mV/V) are shown, respectively,* $\tau_{max}$ *= 5 sec.*

## 4. CONCLUSION

We investigated the solution of TAU transformation using the series expansion inversion method, by using a variant of the inverse technique. The research has demonstrated that the time constant spectrum is successfully determined by this method inverting the field dataset (TDIP). In this research, the inversion has been tested with $\boldsymbol{\tau_{max}}$ = 5, 10 and 15 sec when the number of unknowns varied from *M* = 2 to *M* = 10. It was shown that at $\boldsymbol{\tau_{max}}$ = 5 a total of 3 or 4 main polarization amplitudes can be detected. Also, at $\boldsymbol{\tau_{max}}$ = 10 and 15 sec 3, 4 and 5 main polarization amplitudes can be found. In the series expansion inversion method, based on the fit between the measured and the calculated data it was found that *M* = 2 is a nonphysical solution (*D* = 25.6%), while at *M* = 3 to *M* = 10 the solutions are acceptable (*D* = 6.34% to *D* = 6.64%). It can be shown that the main polarization amplitude is nearly the same at different time constant intervals. The research in the field area demonstrated that 3 or 4 main polarization amplitudes at the relevant characteristic time constants appear at all choices of the number of unknowns.

DHYA19 was drilled in June 2013. The depth of the hole is 210.00 m and the main rocks are cataclastic granite, diorite porphyry, rhyolite, and quaternary sediment. The rocks were very activily altered by silica, silicate, chlorite, and biotite. In the framework of the research, good agreement was found between the result of series expansion based inversion and the lithological information.

## ACKNOWLEDGEMENTS

The research was supported by the European Union, co-financed by the European Social Fund and the GINOP-2.315-2016-00010 *Development of enhanced engineering methods with the aim at utilization of subterranean energy resources* project in the framework of the Széchenyi 2020 Plan, funded by the European Union, co-financed by the European Structural and Investment Funds. I am grateful to the leaders of the Research Institute of Applied Earth Sciences (AFKI), University of Miskolc, Hungary for involving me in the project. Before having been involved in the GINOP project, my PhD studies had been supported by a scholarship of the Mineral Resources Authority of Mongolia (MRAM) of the Government of Mongolia. I would like to thank director Gantumur Kh of the "Noyon Gary" LLC in Mongolia for providing good quality field measured data together with important background information and special geological knowledge about the research area.

## REFERENCES

[1] Keller, G. V., Frischknecht, F. C. (1966). *Electrical Methods in Geophysical Prospecting:* Oxford, Pergamon Press.

[2] Menke, W. (2018). *Geophysical data analysis. Discrete inverse theory*. Elsevier Inc.

[3] Oldenburg, D. W., Li, Y. (1994). Inversion of induced polarization data. *Geophysics*, 59 (9), pp. 1327–1341.

[4] Turai, E., Dobróka, M. (2011). Data processing method developments using TAU-transformation of time-domain IP data I. Theoretical basis. *Acta Geodaetica et Geophysica Hungarica*, 46 (3), pp. 283–290.

[5] Turai, E. (2011). Data processing method developments using TAU-transformation of Time-Domain IP data II. Interpretation results of field measured data. *Acta Geodaetica et Geophysica Hungarica*, 46 (4), pp. 391–400.

[6] Telford, W. M., Telford, W., Geldart, L., Sheriff, R. E., Sheriff, R. E. (1990). *Applied Geophysics*. Cambridge: Cambridge University Press.

[7] Seigel, H. et al. (2007). The early history of the induced polarization method. *The Leading Edge*, 26 (3), pp. 312–321.

[8] Zonge, K. L., Wynn, J. C. (1975). Recent advances and applications in complex resistivity measurements. *Geophysics*, 40 (5), pp. 851–864.

[9] Arifin, M. H. et al. (2019). Data for the potential gold mineralization mapping with the applications of Electrical Resistivity Imaging and Induced Polarization geophysical surveys. *Data in Brief*, 22, pp. 830–835.

[10] Sumner, J. S. (1979). *The induced-polarization exploration method.* Economic Geology, Elsevier Science Inc., pp. 123–133.

[11] Sumner, J. (1976). *Principles of Induced Polariration for Geophysical Exploration: Amsterdam*. Elsevier Science Inc.

[12] Reynolds, J. M. (2011). *An Introduction to Applied and Environmental Geophysics*. John Wiley and Sons. Blackwell, pp. 289–346.

[13] Kearey, P., Brooks, M., Hill, I. (2002). *An Introduction to Geophysical Exploration*. Vol. 4, John Wiley and Sons. Blackwell, pp. 208–230.

[14] Turai, E. (1985). TAU-transformation of time-domain IP curves. *Annales Univ. Scien. Budapestinensis de Rolando Eötvös Nom., Sectio Geophysica et Meteorologica*, Tomus I–II, pp. 182–189.

[15] Dobróka, M., Kis, M., Turai, E. ( 2001). Generalised Series Expansion (GSE) method used in the joint inversion of MT and DC geoelectric data. *Publication of the University of Miskolc, Series A, Mining, Geosciences*, 59, pp. 39–51.

[16] Kiss, A. et al. ( 2016). Laboratory induced polarization data processed with series expansion inversion. *Geosciences and Engineering*, 5 (8), pp. 111–123.

[17] Abordán, A., Szabó, N. P. ( 2020). Uncertainty reduction of interval inversion estimation results using a factor analysis approach. *GEM-International Journal on Geomathematics*, 11 (1), pp. 1–17.

[18] Wait, J. R. (1959). On the electromagnetic response of an imperfectly conducting thin dyke. *Geophysics*, 24 (1), pp. 167–171.